

Clustering, GUT scale and neutrino masses in Ultrahigh energy cosmic rays

ITP Budapest 582

Z. Fodor

Institute for Theoretical Physics, Eötvös University,
Pázmány 1, H-1117 Budapest, Hungary

Abstract. We determine the probability that an ultrahigh energy (above $5 \cdot 10^{19}$ eV) proton created at a distance r with energy E arrives at earth above a threshold E_c . The clustering of ultrahigh energy cosmic rays suggests that they might be emitted by compact sources. We present a statistical analysis on the source density based on the multiplicities. The ultrahigh energy cosmic ray spectrum is consistent with the decay of GUT scale particles. By using a maximum likelihood analysis we determine the mass of these GUT scale particles. We consider the possibility that a large fraction of the ultrahigh energy cosmic rays are decay products of Z bosons which were produced in the scattering of ultrahigh energy cosmic neutrinos on cosmological relic neutrinos. Based on this scenario we determine the required mass of the heaviest relic neutrino as well as the necessary ultrahigh energy cosmic neutrino flux via a maximum likelihood analysis.

1 Introduction

The interaction of protons with the microwave background predicts a drop in the cosmic ray flux above the GZK [1] cutoff $\approx 5 \cdot 10^{19}$ eV. The data shows no such drop. About 20 events even above 10^{20} eV were observed by a number of experiments. Since above the GZK energy the attenuation length of particles is a few tens of megaparsecs if an ultrahigh energy cosmic ray (UHECR) is observed on earth it was most probably produced in our vicinity.

Section 2 studies the propagation and determines the probability $P(r, E, E_c)$ that protons created at distance r with energy E reach earth above a threshold E_c . Using this P one can give the observed spectrum by one numerical integration for any injection spectrum.

It is an interesting phenomenon that the UHECR events are clustered. Usually it is assumed that at these high energies the galactic and extragalactic magnetic fields do not affect the orbit of the cosmic rays, thus they should point back to their origin within a few degrees. In contrast to the low energy cosmic rays one can use UHECRs for point-source search astronomy. Recently, a statistical analysis [2] based on the multiplicities of the clustered events estimated the source density. In Section 3 we extend the above analysis. Our analytical approach gives the event clustering probabilities for any space, intensity and energy distribution of the sources by using a single additional propagation function $P(r, E; E_c)$.

In Section 4 we study the scenario that the UHECRs are coming from decaying superheavy particles (SP) and we determine their masses m_X by an analysis of the observed UHECR spectrum.

Ultrahigh energy neutrinos ($\text{UHE}\nu$) scatter on relic neutrinos ($\text{R}\nu$) producing Z bosons, which can decay hadronically (Z-burst) [3]. In Section 5 we compare the predicted proton spectrum with observations and determine the mass of the heaviest $\text{R}\nu$ via a maximum likelihood analysis.

The details of the presented results and a more complete reference list can be found in [4,5,6].

2 Propagation of UHECR protons

Using pion production as the dominant effect of energy loss for protons at energies $>10^{19}$ eV, ref. [7] calculated $P(r, E, E_c)$ for three threshold energies. We extended the results of [7]. The inelasticity of Bethe-Heitler pair production is small ($\approx 10^{-3}$), thus we used a continuous energy loss approximation for this process. The inelasticity of pion-photoproduction is larger ($\approx 0.2 - 0.5$) in the energy range of interest, thus there are only a few tens of such interactions during the propagation. Due to the Poisson statistics and the spread of the inelasticity, we will see a spread in the energy spectrum even if the injected spectrum is mono-energetic.

In our simulation protons are propagated in small steps (10 kpc), and after each step the energy losses due to pair production, pion production and the adiabatic expansion are calculated. During the simulation we keep track of the current energy of the proton and its total displacement. We used the following type of parametrization $P(r, E, E_c) = \exp[-a \cdot (r/1 \text{ Mpc})^b]$. Fig. 1 shows $a(E/E_c)$ and $b(E/E_c)$ for a range of three orders of magnitude and for five different E_c . Just using the functions of $a(E/E_c)$ and $b(E/E_c)$, thus a parametrization of $P(r, E, E_c)$, one can obtain the observed energy spectrum for any injection spectrum without additional Monte-Carlo simulation.

Since $P(r, E_p; E)$ is of universal usage, we have decided to make the latest numerical data for the probability distribution $(-)\partial P(r, E_p; E)/\partial E$ available for the public via the World-Wide-Web URL

$$\text{http://www.desy.de/~uhecr} .$$

The propagation function can be similarly determined for photons, though the necessary CPU power is approximately 300 times more than for protons. Therefore, we used the stochastic method to test a few cases. Usually the continuous energy loss approximation was used. In this approximation, the energy (and number) of the detected photons is a unique function of the initial energy and distance, and statistical fluctuations are neglected. The processes that are taken into account are pair production on the diffuse extragalactic photon background, double pair production and inverse Compton scattering of the produced pairs. The energy attenuation length of the photons due to these processes is

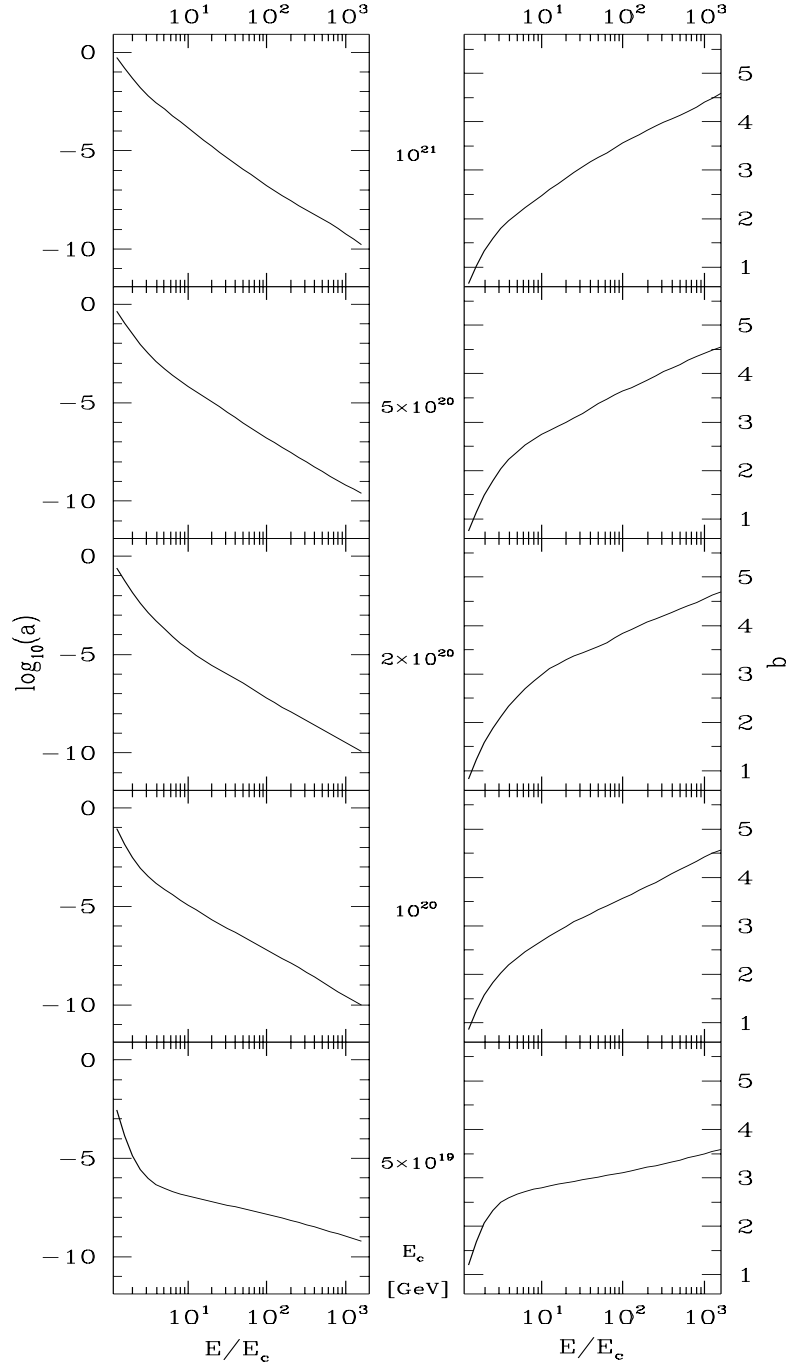


Fig. 1. The parametrization of $P(r, E, E_c)$.

strongly influenced by the poorly known universal radio and infrared backgrounds. These uncertainties influence some of our results.

A full simulation of the photon propagation function with all the statistical fluctuations will be the subject of a later work.

3 Density of sources

The arrival directions of the UHECRs measured by experiments show some peculiar clustering: some events are grouped within $\sim 3^\circ$, the typical angular resolution of an experiment. Above $4 \cdot 10^{19}$ eV 92 cosmic ray events were detected, including 7 doublets and 2 triplets. Above 10^{20} eV, one doublet out of 14 events were found [8]. The chance probability of such a clustering from uniform distribution is rather small [8,9].

The clustered features of the events initiated an interesting statistical analysis assuming compact UHECR sources [2]. The authors found a large number, ~ 400 for the number of sources within the GZK sphere. We generalize their analysis. The most probable value for the source density is really large; however, the statistical significance of this result is rather weak.

The number of UHECRs emitted by a source of luminosity λ during a period T follows the Poisson distribution. However, not all emitted UHECRs will be detected. They might lose their energy during propagation or can simply go to the wrong direction. For UHECRs the energy loss is dominated by the pion production in interaction with the cosmic microwave background radiation. In the previous section the probability function $P(r, E, E_c)$ was calculated.

The features of the Poisson distribution enforce us to take into account the fact that the sky is not isotropically observed.

The probability of detecting k events from a source at distance r with energy E can be obtained by simply including the factor $P(r, E, E_c)A\eta/(4\pi r^2)$ in the Poisson distribution:

$$p_k(\mathbf{x}, E, j) = \frac{\exp[-P(r, E, E_c)\eta j/r^2]}{k!} \times [P(r, E, E_c)\eta j/r^2]^k, \quad (1)$$

where we introduced $j = \lambda T A / (4\pi)$ and $A\eta/(4\pi r^2)$, which is the probability that an emitted UHECR points to a detector of area A . The factor η represents the visibility of the source, which was determined by spherical astronomy. We denote the space, energy and luminosity distributions of the sources by $\rho(\mathbf{x})$, $c(E)$ and $h(j)$, respectively. The probability of detecting k events above the threshold E_c from a single source randomly positioned within a sphere of radius R is

$$P_k = \int_{S_R} dV \rho(\mathbf{x}) \int_{E_c}^{\infty} dE c(E) \int_0^{\infty} dj h(j) \times \frac{\exp[-P(r, E, E_c)\eta j/r^2]}{k!} [P(r, E, E_c)\eta j/r^2]^k. \quad (2)$$

Denote the total number of sources within the sphere of sufficiently large radius (e.g. several times the GZK radius) by N and the number of sources that gave k detected events by N_k . Clearly, $N = \sum_0^\infty N_k$ and the total number of detected events is $N_e = \sum_0^\infty k N_k$. The probability that for N sources the number of different detected multiplets are N_k is:

$$P(N, \{N_k\}) = N! \prod_{k=0}^{\infty} \frac{1}{N_k!} P_k^{N_k}. \quad (3)$$

For a given set of unclustered and clustered events (N_1 and N_2, N_3, \dots) inverting the $P(N, \{N_k\})$ distribution function gives the most probable value for the number

Note, that P_k and then $P(N, \{N_k\})$ are easily determined by a well behaved four-dimensional numerical integration for any $c(E)$, $h(j)$ and $\rho(r)$ distribution functions. In order to illustrate the uncertainties and sensitivities of the results we used a few different choices for these distribution functions.

For $c(E)$ we studied three possibilities. The most straightforward choice is the extrapolation of the ‘conventional high energy component’ $\propto E^{-2}$. Another possibility is to use a stronger fall-off of the spectrum at energies just below the GZK cutoff, e.g. $\propto E^{-3}$. The third possibility is to assume that UHECRs are some decay products of metastable superheavy particles [10,11,12,13,14,15,16,17] or topological defects [18]. The superheavy particles decay into quarks and gluons which initiate multi-hadron cascades through gluon bremsstrahlung [19,20,21,22,23,24].

In the recent analysis [2] the authors have shown that for a fixed set of multiplets the minimal density of sources can be obtained by assuming a delta-function distribution for $h(j)$. We studied both this limiting luminosity, $h(j) = \delta(j - j_*)$, and a more realistic one with Schechter’s luminosity function, which can be given as: $h(j)dj = h \cdot (j/j_*)^{-1.25} \exp(-j/j_*)d(j/j_*)$.

The space distribution of sources can be given based on some particular survey of the distribution of nearby galaxies or on a correlation length r_0 characterizing the clustering features of sources. For simplicity the present analysis deals with a homogeneous distribution of sources.

In order to determine the confidence level (CL) regions for the source densities we used the frequentist method [25]. We wish to set limits on S , the source density. Using our Monte-Carlo based $P(r, E, E_c)$ functions and our analytical technique we determined $p(N_1, N_2, N_3, \dots; S; j_*)$, which gives the probability of observing N_1 singlet, N_2 doublet, N_3 triplet etc. events if the true value of the density is S and the central value of luminosity is j_* . For a given set of $\{N_i, i = 1, 2, \dots\}$ the above probability distribution as a function of S and j_* determines the 68% and 95% confidence level regions in the $S - j_*$ plane.

Fig. 2 shows the confidence level regions for one of our models (with injected energy distribution $c(E) \propto E^{-3}$; and Schechter’s luminosity distribution: $h(j)dj \propto (j/j_*)^{-1.25} \exp(-j/j_*)d(j/j_*)$). The regions are deformed, thin ellipse-like objects. For this model our final answer for the density is $180^{+2730(8817)}_{-165(174)} \cdot 10^{-3} \text{ Mpc}^{-3}$, where the first errors indicate the 68%, the second ones in the

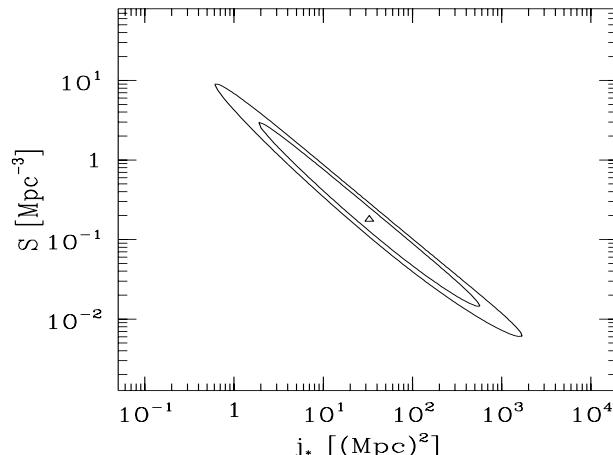


Fig. 2. The 1σ (68%) and 2σ (95%) confidence level regions for j_* and the source density (14 UHECR with one doublet).

parenthesis the 95% CLs, respectively. The choice of $[2] -h(j) \propto \delta(j)-$ and, e.g. E^{-2} energy distribution gives much smaller value: $2.77^{+96.1(916)}_{-2.53(2.70)} 10^{-3} \text{ Mpc}^{-3}$, which is in a quite good agreement with the result of Ref. [2].

4 Decay of GUT scale particles

An interesting idea discussed by refs.[15,16,17] is that SPs could be the source of UHECRs. Note, that any analysis of SP decay covers a much broader class of possible sources. Several non-conventional UHECR sources produce the same UHECR spectra as decaying SPs. We study the scenario that the UHECRs are coming from decaying SPs and we determine the mass of this X particle m_X by a detailed analysis of the observed UHECR spectrum.

The hadronic decay of SPs yields protons. They are characterized by the fragmentation function (FF) $D(x, Q^2)$ which gives the number of produced protons with momentum fraction x at energy scale Q . For the proton's FF at present accelerator energies we use ref. [26]. We evolve the FFs in ordinary and in supersymmetric QCD to the energies of the SPs. This result can be combined with the prediction of the MLLA technique, which gives the initial spectrum of UHECRs at the energy m_X (cf. Fig.. 3). Similar results are obtained by [27].

Depending on the location of the source –halo or extragalactic (EG)– and the model –SM or MSSM– we study four different scenarios. In the EG case protons lose some fraction of their energies, described by $P(r, E, E_c)$. We compare the predicted and the observed spectra by a maximum likelihood analysis. This analysis gives the mass of the SP and the error on it.

Fig. 4 shows the measured UHECR spectrum and the best fit, which is obtained in the EG-MSSM scenario.

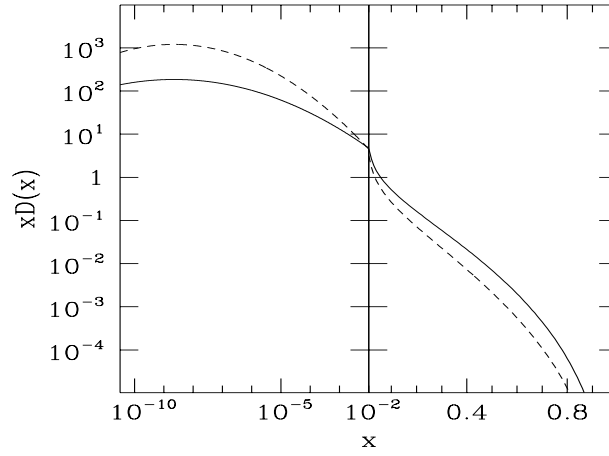


Fig. 3. The quark FFs at $Q=10^{16}$ GeV for proton/pion in SM (solid/dotted line) and in MSSM (dashed/dashed-dotted line). We change from logarithmic scale to linear at $x = 0.01$.

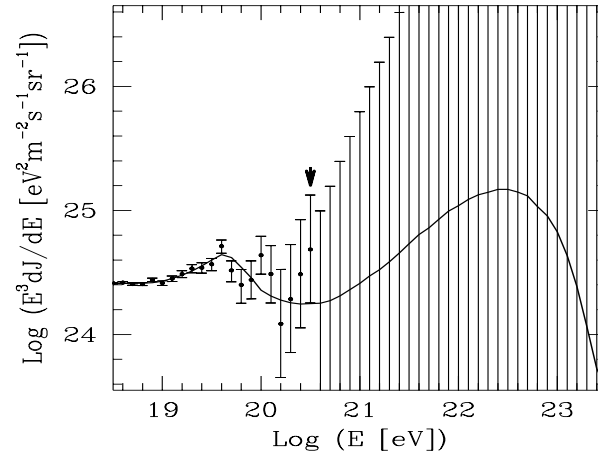


Fig. 4. UHECR data with their error bars and the best fit from a decaying SP. There are no events above 3×10^{20} eV (shown by an arrow). Zero event does not mean zero flux, but an upper bound for the flux. Thus, the experimental flux is in the "hatched" region with 68% CL.

To determine the most probable value for the mass of the SP we studied 4 scenarios. Fig. 5 contains the χ^2_{min} values and the most probable masses with their errors for these scenarios.

The UHECR data favors the EG-MSSM scenario. The goodnesses of the fits for the halo models are far worse.

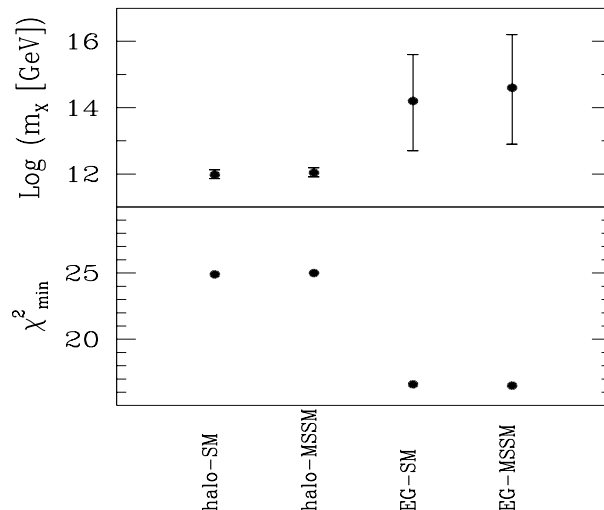


Fig. 5. The most probable values for the mass of the decaying ultra heavy dark matter with their error bars and the total χ^2 values. Note that 21 bins contain nonzero number of events and the fit has 3 free parameters.

The SM and MSSM cases do not differ significantly. The most important message is that the masses of the best fits (EG cases) are compatible within the error bars with the MSSM gauge coupling unification GUT scale: $m_X = 10^b$ GeV, where $b = 14.6^{+1.6}_{-1.7}$.

5 Z-burst scenario

Already in the early eighties there were some discussions about the possibility that the ultrahigh energy neutrino spectrum could have absorption dips at energies around $E_{\nu_i}^{res} = M_Z^2 / (2m_{\nu_i}) = 4.2 \cdot 10^{21}$ (1 eV/ m_{ν_i}) eV due to resonant annihilation with relic neutrinos of mass m_ν , predicted by the hot Big Bang, into Z bosons of mass M_Z [28,29]. Recently it was realized that the same annihilation mechanism gives a possible solution to the GZK problem [3]. It was argued that the UHECRs above the GZK cutoff are from these Z-bursts. The Z-burst hypothesis for the ultrahigh energy cosmic rays was discussed in many papers [30,31,32,10,33,11,34,35,36,6,37,38,39].

We compare this scenario with observations.

The density distribution of $R\nu$ s as hot DM follows the total mass distribution; however, it is less clustered. Thus we, as opposed to practically all previous authors [3,31,30], do not follow the unnatural assumption of having a relative overdensity of $10^2 \div 10^4$ in our neighborhood (for an approach with lepton asymmetry see [32]). Our quantitative results turned out to be rather insensitive to the variations of the overdensities within the considered range.

We give the energy distribution of the produced particles in our lab system, which is obtained by Lorentz transforming the CM collider results. We included in our analysis the protons, which are directly produced in the Z-burst and appear as decay products of the neutrons. Photons were also taken into account. They are produced in hadronic Z decays via fragmentation into neutral pions, $Z \rightarrow \pi^0 + X \rightarrow 2\gamma + X$. Electrons (and positrons) from hadronic Z decay are also relevant for the development of electromagnetic cascades. They stem from decays of secondary charged pions, $Z \rightarrow \pi^\pm + X \rightarrow e^\pm + X$.

The UHECR flux from Z-bursts is proportional to the differential fluxes F_{ν_i} of ultrahigh energy cosmic neutrinos. Unfortunately, the value of these fluxes is essentially unknown. In this situation of insufficient knowledge, we take the following approach concerning the flux of ultrahigh energy cosmic neutrinos of type i , $F_{\nu_i}(E_{\nu_i}, r)$. It is assumed to have the form

$$F_{\nu_i}(E_{\nu_i}, r) = F_{\nu_i}(E_{\nu_i}, 0) (1 + z)^\alpha, \quad (4)$$

where z is the redshift and where α characterizes the cosmological source evolution. Note, however, that, independently of the production mechanism, neutrino oscillations result in a uniform mixture for the different mass eigenstates.

The next ingredient of our analysis is the propagation of the protons and photons from cosmological distances. This propagation was described by the appropriate $P(r, E_p, E)$ probability functions (see Section 2).

Finally, we compare the predicted and observed spectrum and extract the mass of the relic ν and the necessary UHE ν flux by a maximum likelihood analysis. Qualitatively, our analysis can be understood as follows. In the Z-burst scenario small relic ν mass needs large E_ν^{res} to produce a Z. Large E_ν^{res} results in a large Lorentz boost, thus large proton energy. In this way the detected energy determines the mass of the relic ν . The analysis is completely analogous to that of the previous section. The observed flux is a sum of two terms, namely the flux from Z-bursts and a conventional part with power-law behaviour in the energy. This power-law part might be produced in our galaxy (halo model) or it might be produced extragalactically (EG model).

The Z-burst determination of the neutrino mass seems reasonably robust. Fig. 6 shows the summary of our relic neutrino mass determination. For a wide range of cosmological source evolution ($\alpha = -3 \div 3$), Hubble parameters $h = 0.61 \div 0.9$, Ω_M , Ω_Λ , $z_{\text{max}} = 2 \div 5$, for variations of the possible relic neutrino overdensity in our GZK zone and for different assumptions about the diffuse extragalactic photon background, the results remain within the above error bars. The main uncertainties concerning the central values originate from the different assumptions about the background of ordinary cosmic rays.

In the case that the ordinary cosmic rays above $10^{18.5}$ eV are protons and originate from a region within the GZK zone of about 50 Mpc (“halo”), the required mass of the heaviest neutrino seems to lie between $2.1 \text{ eV} \leq m_\nu \leq 6.7 \text{ eV}$ at the 68% C.L. ($\alpha \leq 0$), if we take into account the variations between the minimal and moderate universal radio background cases and the strong UHE γ attenuation case.

The much more plausible assumption that the ordinary cosmic rays above $10^{18.5}$ eV are protons of extragalactic origin leads to a required neutrino mass of $0.08 \text{ eV} \leq m_\nu \leq 1.3 \text{ eV}$ at the 68% C.L. ($\alpha \leq 0$). In this case the predicted mass has a relatively strong dependence on the value of the universal radio background. Physically it is easy to understand the reason. The small radio background leads to a relatively large UHE γ fraction in the observations. They do not lose that much energy. Thus, smaller incoming UHE ν energy and larger m_ν is needed to describe the data.

We performed a Monte Carlo analysis studying higher statistics. In the near future, the Pierre Auger Observatory will provide a ten times higher statistics, which reduces the error bars in the neutrino mass to about one third of their present values.

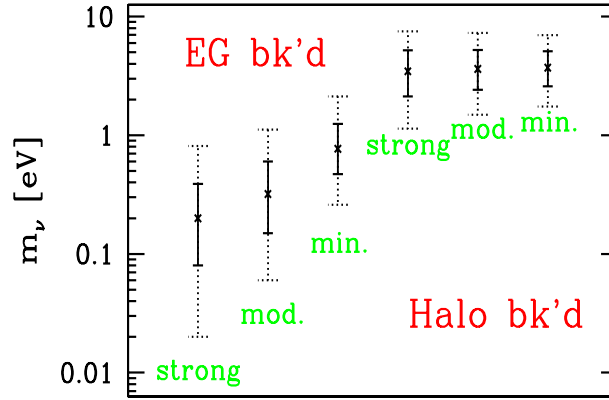


Fig. 6. Summary of the masses of the heaviest neutrino required in the Z-burst scenario, with their 1σ (solid) and 2σ (dotted) error bars, for the case of an extragalactic and a halo background of ordinary cosmic rays and for various assumptions about the diffuse extragalactic photon background in the radio band ($\alpha = 0, h = 0.71, \Omega_M = 0.3, \Omega_A = 0.7, z_{\max} = 2$). From left: strong γ attenuation, moderate and minimal universal radio background.

It should be stressed that, besides the neutrino mass, the UHE ν flux at the resonance energy is one of the most robust predictions of the Z-burst scenario which can be verified or falsified in the near future. The required flux of ultrahigh energy cosmic neutrinos near the resonant energy should be detected in the near future by AMANDA, RICE, and the Pierre Auger Observatory, otherwise the Z-

burst scenario will be ruled out (cf. Fig. 7). If such tremendous fluxes of ultrahigh energy neutrinos are indeed found, one has to deal with the challenge to explain their origin. It is fair to say, that at the moment no convincing astrophysical sources are known which meet the requirements for the Z-burst hypothesis, i.e. which have no or a negative cosmological evolution, accelerate protons at least up to 10^{23} eV, are opaque to primary nucleons and emit secondary photons only in the sub-MeV region. It is an interesting question whether such challenging conditions can be realized in BL Lac objects, a class of active galactic nuclei for which some evidence of zero or negative cosmological evolution has been found (see Ref. [41] and references therein) and which were recently discussed as possible sources of the highest energy cosmic rays [42].

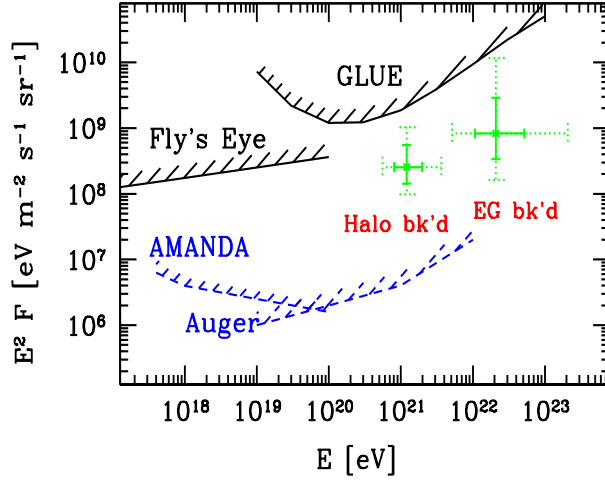


Fig. 7. Neutrino fluxes, $F = \frac{1}{3} \sum_{i=1}^3 (F_{\nu_i} + F_{\bar{\nu}_i})$, required by the Z-burst hypothesis for the case of a halo and an extragalactic background of ordinary cosmic rays, respectively ($\alpha = 0, h = 0.71, \Omega_M = 0.3, \Omega_\Lambda = 0.7, z_{\max} = 2$). Shown are the necessary fluxes obtained from the fit results for the case of a strong UHE γ attenuation. The horizontal errors indicate the 1σ (solid) and 2σ (dotted) uncertainties of the mass determination and the vertical errors include also the uncertainty of the Hubble expansion rate. Also shown are upper limits from Fly's Eye on $F_{\nu_e} + F_{\bar{\nu}_e}$ and the Goldstone lunar ultrahigh energy neutrino experiment GLUE on $\sum_{\alpha=e,\mu} (F_{\nu_\alpha} + F_{\bar{\nu}_\alpha})$, as well as projected sensitivities of AMANDA on $F_{\nu_\mu} + F_{\bar{\nu}_\mu}$ and Auger on $F_{\nu_e} + F_{\bar{\nu}_e}$. The sensitivity of RICE is comparable to the one of Auger.

The nice collaboration with S.D. Katz and A. Ringwald and the careful reading of the manuscript is acknowledged. This work was partially supported by Hung. Sci. grants No. OTKA-T37615T34980/T29803/M37071M28413/OM-MU-708/OMFB-1548.

References

1. K. Greisen, Phys. Rev. Lett. **16** (1966) 748; G.T. Zatsepin and V.A. Kuzmin, Pisma Zh. Exp. Teor. Fiz. **4** (1966) 114.
2. S.L. Dubovsky, P.G. Tinyakov and I.I. Tkachev, Phys. Rev. Lett. **85** (2000) 1154.
3. D. Fargion, B. Mele, A. Salis, Astrophys. J. **517** (1999) 725; T.J. Weiler, Astropart. Phys. **11** (1999) 303; **12** (2000) 379 (Erratum). See also e.g.: T.J. Weiler, hep-ph/0103023; D. Fargion et al., hep-ph/0112014.
4. Z. Fodor, S.D. Katz, Phys. Rev. D **63** (2001) 023002; hep-ph/0105347.
5. Z. Fodor, S.D. Katz, Phys. Rev. Lett. **86** (2001) 3224; hep-ph/0105348.
6. Z. Fodor, S.D. Katz, and A. Ringwald, Phys. Rev. Lett. **88** (2002) 171101; hep-ph/0105336; hep-ph/0203198, A. Ringwald, hep-ph/0111112.
7. J.N. Bahcall and E. Waxman, Astrophys. J. **542** (2000) 543.
8. Y. Uchihori et al., Astropart. Phys. **13** (2000) 151.
9. N. Hayashida et al., Phys. Rev. Lett. **77** (1996) 1000.
10. G. Gelmini and A. Kusenko, Phys. Rev. Lett. **84** (2000) 1378.
11. J. L. Crooks, J. O. Dunn and P. H. Frampton, Astrophys. J. **546** (2001) L1.
12. J. R. Ellis, J. L. Lopez and D. V. Nanopoulos, Phys. Lett. B **247** (1990) 257.
13. J. R. Ellis, G. B. Gelmini, J. L. Lopez, D. V. Nanopoulos and S. Sarkar, Nucl. Phys. B **373** (1992) 399.
14. P. Gondolo, G. Gelmini, and S. Sarkar, Nucl. Phys. B **392** (1993) 111.
15. V. Berezhinsky, M. Kachelrieß and A. Vilenkin, Phys. Rev. Lett. **79** (1997) 4302.
16. V.A. Kuzmin, V.A. Rubakov, Phys. Atom. Nucl. **61** (1998) 1028.
17. M. Birkel and S. Sarkar, Astropart. Phys. **9** (1998) 297; S. Sarkar, hep-ph/0005256.
18. V. S. Berezhinsky and A. Vilenkin, Phys. Rev. D **62** (2000) 083512.
19. V. Berezhinsky and M. Kachelrieß, Phys. Lett. B **434** (1998) 61.
20. V. Berezhinsky and M. Kachelrieß, Phys. Rev. D **63** (2001) 034007.
21. R. Toldra, Comput. Phys. Commun. **143** (2002) 287.
22. R. Toldra, astro-ph/0201151.
23. C. Barbot and M. Drees, hep-ph/0202072.
24. A. Ibarra and R. Toldra, hep-ph/0202111.
25. D. Groom *et al.*, Eur. Phys. J. C **15** (2000) 1.
26. J. Binnenwies, B.A. Kniehl, G. Kramer, Phys. Rev. D **52** (1995) 4947;
27. S. Sarkar and R. Toldra, hep-ph/0108098; R. Toldra, hep-ph/0108127.
28. T.J. Weiler, Phys. Rev. Lett. **49** (1982) 234; E. Roulet, Phys. Rev. D **47** (1993) 5247.
29. S. Yoshida *et al.*, Astrophys. J. **479** (1997) 547.
30. E. Waxman, astro-ph/9804023; J.J. Blanco-Pillado et al., Phys. Rev. D **61** (2000) 123003.
31. S. Yoshida, G. Sigl, and S. Lee, Phys. Rev. Lett. **81** (1998) 5505.
32. G. Gelmini and A. Kusenko, Phys. Rev. Lett. **82**, 5202 (1999).
33. T. J. Weiler, hep-ph/9910316.
34. G. B. Gelmini, hep-ph/0005263.
35. H. Päs and T. J. Weiler, Phys. Rev. D **63** (2001) 113015.
36. D. Fargion, M. Grossi, P. G. De Sanctis Lucentini, C. Di Troia and R. V. Konoplich, astro-ph/0102426.
37. B. H. McKellar, M. Garbutt, G. J. Stephenson and T. Goldman, hep-ph/0106123.
38. O. E. Kalashev, V. A. Kuzmin, D. V. Semikoz and G. Sigl, hep-ph/0112351.
39. G. Gelmini and G. Varieschi, hep-ph/0201273.
40. P. Sreekumar *et al.*, Astrophys. J. **494** (1998) 523.
41. A. Caccianiga *et al.*, astro-ph/0110334.
42. P. G. Tinyakov and I. I. Tkachev, astro-ph/0102476.